

Optical Distributed Sensing: Reel-To-Reel Fabrication of Quasi-Distributed FBGs for Improved Scattering Signal and Enhanced Harsh Environment Stability

by

Shuda Zhong

Bachelor of Engineering, University of Nottingham Ningbo China, 2019

Submitted to the Graduate Faculty of the
Swanson School of Engineering in partial fulfillment
of the requirements for the degree of
Master of Science

University of Pittsburgh

2021

UNIVERSITY OF PITTSBURGH

SWANSON SCHOOL OF ENGINEERING

This thesis was presented

by

Shuda Zhong

It was defended on

April 1, 2021

and approved by

Kevin P. Chen, Ph.D., Professor, Department of Electrical and Computer Engineering

Zhi-Hong Mao, Ph.D., Professor, Department of Electrical and Computer Engineering

Liang Zhan, Ph.D., Assistant Professor, Department of Electrical and Computer Engineering

Thesis Advisor: Kevin P. Chen, Ph.D., Professor, Department of Electrical and Computer Engineering

Copyright © by Shuda Zhong

2021

Optical Distributed Sensing: Reel-to-Reel Fabrication of quasi-distributed FBGs for Improved scattering signal and enhanced harsh environment stability

Shuda Zhong, M.S.

University of Pittsburgh, 2021

Bragg gratings inscribed in optical fiber are key components for both multiplexable and distributed optical sensing. Comparing with other sensor devices, Bragg grating based fiber sensors offer a number of advantages include low manufacturing cost, immunity to electromagnetic fields (IMFs), long lifetimes, high sensitivity, multiplexing, and environmental ruggedness. Bragg grating based fiber sensor arrays have been used extensive to perform structural health monitoring for large civil and mechanic structures. To perform high spatial resolution measurements on large structures, thousands of grating devices need to be multiplexed on a single fiber.

In this thesis, a fully automated reel-to-reel fiber handling system is designed and integrated into a KrF 248-nm excimer laser, enabling continuous Bragg grating fabrication using a phase mask approach. Through the control of fiber tension and spooling speed, grating sensor can be inscribed continuously at desired locations within 5-mm accuracy. One hundred fifty evenly spaced FBGs have been successfully inscribed in a single fiber with 3-cm spacing, spectral and spatial characteristics of these fiber sensors are characterized using an Optical Backscatter Reflectometry (OBR). The spectral accuracy was within 0.5-nm of the designed grating wavelength, which are sufficient for both optical time domain reflectometry and optical frequency domain reflectometry interrogation. The successful development of this fully automated grating fabrication system enable development of fiber sensing cables for a wide array of applications.

Table of Contents

Acknowledgment.....	viii
1.0 Introduction.....	1
1.1 Background and Motivation.....	1
1.2 Thesis Contribution.....	4
1.3 Thesis Outline	5
2.0 Fiber Bragg Grating	7
2.1 Optical Fiber Sensors	7
2.2 Optical Fiber Grating.....	11
2.3 FBG Technology	15
2.4 Interrogation Techniques and Multiplexing for Quasi-Distributed FBGs	18
3.0 Reel to Reel System Design and Working Principle	21
3.1 Components and Layout.....	21
3.2 Control Algorithm and Fabrication Process.....	28
3.3 Fabrication Results.....	31
4.0 Summary and Future Works.....	34
4.1 Summary	34
4.2 Future Works.....	35
Bibliography	37

List of Tables

Table 1. Various grating profiles.....	12
---	-----------

List of Figures

Figure 1 . Grating profile fabrication process.....	4
Figure 2. Fiber structure and light propagation process	11
Figure 3. Spectra of an FBG	13
Figure 4. Reel-to-reel system components	21
Figure 5. Reel-to-reel system layout	22
Figure 6. Ferrule structure.....	24
Figure 7. Top view of the fiber drawing displacement testing monitored by camera.....	25
Figure 8. 3D printing flange with its cross-section view.....	26
Figure 9. Reel-to-reel system communication setup	28
Figure 10. Circuitry of the motor driver	29
Figure 11. Reel-to-reel system control algorithm.....	30
Figure 12. OBR scanning result.....	32
Figure 13. Peak wavelength of the fabricated sample	33
Figure 14. Corresponding reflectivity of the fabricated sample.....	33
Figure 15. Combination of peak wavelength with corresponding reflectivity of the fabricated sample.....	33

Acknowledgment

First of all, I would like to express my sincere gratitude to my advisor, Professor Kevin Chen, for his patience, encouragement, guidance, and support throughout the study of my master program. His firm commitment to research and hard work are two motivating factors that kept me going through out my masters' and gain immense knowledge both practically and theoretically. I would also like to thank my committee member Professor Zhi-Hong Mao and Professor Liang Zhan for their guidance and support.

Secondly, I would like to thank Jingyu Wu for her detailed guidance and useful suggestions. I owe special gratitude to Kehao Zhao and Yuqi Li for so many inspiring suggestions to this work. I also want to thank Dr. Mohan Wang, and Jieru Zhao for so much beneficial discussion.

Last but not least, I want to express my deep gratitude to my parents, sister and friends for believing in me and for their unfailing support and continuous encouragement.

1.0 Introduction

In this section, we will present the background and motivation in Section 1.1, the thesis contribution in Section 1.2, and thesis outline in Section 1.3.

1.1 Background and Motivation

Rayleigh-based distributed optical fiber sensors (DOFSs) have attracted tremendous attention due to their capability of detecting changes in strain, acoustics, temperature, pressure, corrosion, relative humidity, viscosity, chemical concentration, radiation, and a host of other measurands. These sensors have the most prominent potential in applications of structural health monitoring such as oil and gas pipelines leakage monitoring, down-hole sensing in oil wells, and for intrusion detection., etc.

In distributed optical fiber sensing based on Rayleigh scattering, coherent laser pulses are sent along the optical fiber, and the optical fiber act as a distributed interferometer as a result of Rayleigh scattering along the optical fiber, and a gauge length approximately equal to the pulse length can be observed. After the laser pulse is sent to the optical fiber, the intensity of the reflected light will be measured as a function of time. Therefore, perturbation of a certain section of fiber will induce changes in the reflected intensity of successive pluses from the corresponding region of fiber. However, the resolution and sensitivity of DOFS are restricted in conventional optical fibers due to low Rayleigh scattering intensity.

To solve the low Rayleigh scattering problem, different methods have been studied. One approach is via improving the capture efficiency for backscattered light from more numerical aperture (NA) of the fiber. However, in the actual design space of single-mode fiber, the increase in capture efficiency is less than 2 dB. Another method is to add scattering particles, but more scattering particles usually increases the fiber attenuation. One approach to increase the optical backscattering involves laser processing of optical fiber. Exposing optical fibers to pulsed radiation is well known to increase Rayleigh scattering. Backscattering can be further increased by forming periodic or quasi-periodic Bragg gratings. The Bragg grating can be inscribed along a fiber of great lengths while the attenuation of the fiber does not significantly increase.

To fabricate periodic gratings over a long length of optical fiber, one method is to expose the optical fiber to the UV light while fiber is drawing, and coating is applied after the UV exposure, but this method has problem aligning the fiber with the laser system while the fiber is drawing, particularly the vibration from drawing process is inevitable. Another approach is to firstly remove the coating, then expose the fiber to UV light, finally recoating the fiber for protection. However, this method would cause waste for original fiber coating, furthermore, the glass surface of the fiber might be damaged by the coating removal process, causing fiber reliability issues. Improvements in the above aspects are desirable. Therefore, the present approach has developed a small-diameter single-mode optical fiber with grating and its forming process.

The fabrication of periodic or quasi-periodic Bragg gratings over a long length of optical fiber requires higher standard and more labor when compared to traditional single point sensors fabrications. The limitation on manual fabrication of quasi-distributed FBGs lies in precision, speed, and distance.

In general, a single FBG point sensor can be fabricated by a UV laser using a phase mask as shown in the Figure 1, or a femtosecond laser via point-by-point procedure to form the desired grating profile into the fiber.

The phase mask is made of a silicon glass plate, which is transparent to UV rays. On one of the planes, photolithography is used to etch a one-dimensional periodic surface relief structure, causing transparent and opaque regions. The shape of the periodic pattern is approximately a square wave in profile. To fabricate Bragg gratings using a UV laser with a phase mask, the optical fiber is placed almost in contact with the profile of the phase mask. When the optical fiber is exposed to light through the phase mask, the photosensitive effect causes the fiber core to produce a periodic grating structure which changes the refractive index of the core. To use a femtosecond laser to fabricate Bragg gratings, first, the femtosecond pulsed laser is focused on the fiber core through the polyimide coating and the fiber cladding, and then uniformly spaced lines are carved on the core and cladding using a plane-by-plane method.

No matter which methods is used to fabricate an FBG, the fiber needs to be precisely aligned to meet the laser pulse. To inscribe the FBG to the fiber successfully, the fiber needs to be within the working range of the laser, which could be as small as a quarter of the diameter of fiber core. Apart from that, the tension of the fiber needs to be in constant during the photo imprinting process since the FBG reflective wavelength will be shifted if the tension is changed. Furthermore, it is cumbersome to fabricate FBGs manually while ensure each sensing point is evenly distributed, meanwhile, handling and fixing the fiber to the laser targeting position reduce the speed of fabrication significantly and would break the fiber because it is fragile, and the number of FBGs that can be inscribed along one optical fiber is limited by manual fabrication because as the length

of fiber increase, the collection and handling of fiber would be more vulnerable to bending and breaking off.

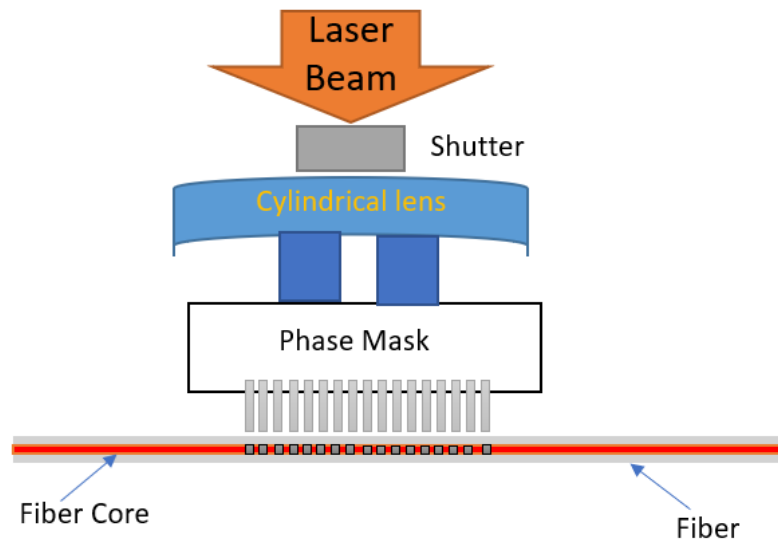


Figure 1 . Grating profile fabrication process

1.2 Thesis Contribution

In this thesis, two major works are done regarding the fabrication and testing of quasi-distributed FBG sensors: One aims at developing a reel-to-reel system that significantly improve the efficiency and accuracy of quasi-distributed FBG sensors fabrication using the small diameter single-mode optical fiber in [1], while the other focuses on testing the fabricated sensor via OBR.

Firstly, to address the problem lies in manual fabrication of quasi-distributed fiber sensors, a fully automated reel-to-reel system is designed and integrated into the laser system, allowing evenly spaced gratings to be inscribed continuously along an optical fiber. The system consists of two motors, fiber guidance, alignment and supports, two spools for fiber feeding and collection, and a control center (computer). The speed and distance are controllable via LabVIEW.

Meanwhile, to attain stable tension, the motor is controlled to have steady acceleration and deceleration to overcome the effect of momentum. The reel-to-reel system is tested and 150 FBGs are inscribed along a single fiber using this system. Total time consumed is less than an hour, therefore, the speed limitations of manual fabrication is removed. Since two large spools are used for fiber feeding and collection, the length of the fiber does not affect the handling risk of breaking off the fiber, the distance limit is also transcended.

Furthermore, the samples fabricated by the reel-to-reel system is then scanned by OBR, the results indicate each FBG are spaced evenly with three centimeters, and their Bragg waveforms are very closed, which proves that the precision limitations of manual fabrication is also overcome.

1.3 Thesis Outline

This thesis consists of five chapters and is organized as follows:

Chapter 1 states the background, motivation, and contributions of this thesis.

Chapter 2 describes the basic techniques for fiber optic sensor fabrication, their characteristics, and the fundamental properties of fiber gratings, A focus is given on FBG and quasi-distributed FBG where fundamental theory, working principles and limitations are discussed.

Chapter 3 proposes the design of a fully automated reel-to-reel system to solve the problem inherent in manual fabrication of FBGs. The components layout, control algorithms, fabrication process and results are provided and the goal of fabricating an extended quasi-distributed FBGs is achieved.

Chapter 4 concludes all the work in this thesis and proposes possible approaches to improve performance and further applications of the reel-to-reel for future research.

2.0 Fiber Bragg Grating

In this section, we will present the fiber optic sensors' working principle and basic composition in Section 2.1, the principle of fiber Bragg gratings in Section 2.2, FBG technology in Section 2.3, and the interrogation techniques and multiplexing for quasi-distributed FBGs in Section 2.4.

2.1 Optical Fiber Sensors

In the past few decades, extensive research in the fields of optoelectronics and optical fiber communications has increased dramatically. As a result, applications were initially concentrated on military and aerospace equipment, and later on heritage culture [2], medical health monitoring [3], [4], and various engineering fields [5-8]. More recently, devices like laser printers, small volume disc-players, and laser Pointers, barcode scanners have been brought by the optoelectronics industry. More stable and higher performance telecommunication links with reducing bandwidth cost have been provided by the fiber optic communication industry, particularly the advancement in both fiber optical communication and optoelectronics were applied in the broad study of optic sensor (FOS) technology. The development and subsequent mass production of components in FOS technology has been in turn applied in these industries [9], [10]. Joint developments optimize the components with lower prices and replace conventional electrical sensing device for acceleration, rotating movement, temperature, corrosion, compression force,

acoustics, crack formation, vibration, linear and angular position, humidity, strain, chemical material measurements, viscosity, and many other sensing deployments[11].

Generally, ‘A-to-E’ characteristics are required for a effective and reliable sensory technology which can used in a high-performance monitoring system as listed follow: (A)ccuracy: sensor is expected to be stably accurate; (B)enefit: sensor is expected to be competitive in commercial price with acceptable cost; (C)ompact: the size of the sensor is expected to be small, especially for embedment application; (D)urable: sensor is expected to have a long service life; and (E)asy: straightforward to handle with the time it takes to retrieve the sensing information should be as fast as almost at the same time [12]. Therefore, the optical fiber sensors features adequately meets these requirements that the FOS can be used intrinsically or extrinsically depends on applications.

Inherent optical sensors use optical fibers directly as sensing materials and as a way to transmit optical signals that interfere with environmental data. The light would be contained in the optical fiber and conduct sensing function, in this case, other than at the detecting end of the sensor. While as for external sensors, the optical fiber is directly applied to be a light carrying device that goes to and from the optical sensor head location. Externally located, the sensor head typically uses optical elements, and is required to modulate the characteristics of light changes induced by the physical disturbance of the target in the environment. Inherent fiber optic sensor are more appealing and have been extensively studied, because compared with the external, this solution has many advantages, for example, the fiber sensor head design adaptability and their inner fiber characteristics [13].

The signal transmission method and main carrier in optical fibers (OFs) are photons, which hold no electrical charges, and therefore is unbiased in electrical field. A photons has no mass in

while no moving. Compared with electrons, in movement, their weight is close to zero. In wires, electrons need to receive a voltage as a pushing to transcend the initial momentum and thus can moves, when electrons flows, it forms current in the wire, generating heat. In addition, the magnetic field generated by the electron flow exceeds the wire boundary. Such fields interfere with the current in other conductors within the field, and unwanted current might be generated in the conductors according to Faraday's theory. The field generated by the current might be undesired that causing crosstalk among the conductors, resulting in interference in sensor performance. In addition, the conducting wires would draw flashing spark that render equipment failure inoperative [14] or the sensor reverses in the presence of other factors.

However, with the application of the FOS system, photons have none of these conditions. Photon even generate no electrical or electromagnetic fields within one optical fibre, therefore, it can dramatically removing the cross-talk. Unlike two adjacent electrons traveling in the same wire, there is no interaction between two adjacent photons traveling in the same fiber. As a result, multiple conductors is not able to combine and form to one conductor to prevent the electron from being repelled because of electrons' universal charge. In contrast, the combination of an extremely huge amount of information into one optical fiber is possible, this configuration names multiplication. Because the fiber does not carry any electrical signals, it is safer in harsh environments such as those containing explosive gases or fuels. Size and weight may not be essential in certain applications, but they can be crucial in others, and reducing them can be very useful [15], [16].

A fiber is basically a glass or plastic solid string that carries light along its length. Fiber sensors are sensitive to any factor that alters the frequency, polarization, intensity, or light phase that passes across the fiber. The feasibility to investigate multiple sensing elements multiplexable

[17-20] within one fiber makes it possible to equip a whole structure by using the optical sensor and controllable quantity of accessing and processing centers. It allows signal to be transmitted across greater length with larger band-width comparing with other communication mode. Signals travel more efficiently through fibers than through metal wires. Optical fiber is used instead of metal wires for signal transmission since it has less signal loss.

As shown in Figure 2, the basic fiber structure required for the guidance of the light wave has a core surrounded by cladding. The total internal reflection of pulse that occurs at the region of interface between cladding and core is used to propagate light down an OF. The cladding's lower refractive index refracts light, which keeps it contained in the fiber. Figure 2 shows a cross-section of a typical OF. OFs are fiber strands made up of cores and cladding of distinct refractive indices. The refractive index of the cladding of an OF is lower than that of the core, so that light propagates down the core instead of escaping. When light travels through the medium at a specific angle of incidence, total internal reflection occurs. The propagation of light within an OF is represented in Figure 2, where θ_a , θ_b and θ_c are distinct propagation angles. The reflecting pulse with angle θ_b flows approximately around core-cladding interface. Between the refracted light path and the regular light path, a 90-degree angle is created. When the incident angle of light is larger than the critical angle, the light is reflected into the core which enable the pulse to pass into the fiber core and is confined by the fiber cladding [21].

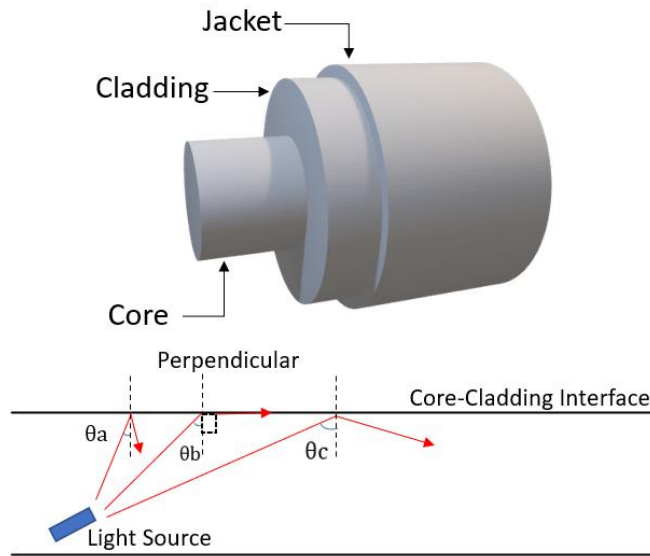





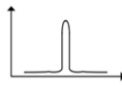
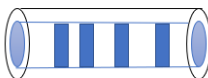


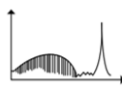


Figure 2. Fiber structure and light propagation process

2.2 Optical Fiber Grating

Fiber gratings [22] are periodic perturbation of the core refractive index of an optical fiber. These sensors can be categorized into two groups based on the grating period (Λ): If Λ is on the order of m , it is Fiber Bragg Grating (FBG); if Λ is several hundreds of m , it is Long Period Grating (LPG). Imprinting different grating profiles is possible owing to phase masking. The pulse passes through the gratings is heavily influenced by grating profiles. Because the grating profile configuration located in the OF core has such a large impact on light wavelength modulation, the performance of various grating profiles in sensing has been considered and studied. The illustration of each grating profile is shown in **Table 1**.

Table 1. Various grating profiles

Grating Profiles	Grating Structure	Reflective Spectrum	Reference
Uniform Grating			[46]
Long Period Grating			[46]
Apodized Grating			[47]
Chirped Grating			[48]
Tilted Grating			[49], [50]

Their operation uses the interaction of a core transmission mode with different core or cladding modes. [23] specifies phase-matching condition that must be met as follow:

$$\Delta\beta = \frac{2\pi}{\Lambda} m \quad (2.1)$$

where the subtraction of the involved modes' propagation indexes is denoted by the letter $\Delta\beta = \beta_1 - \beta_2$. The integer m is referred to as the mode order, $m = 1$ otherwise the waveguide support more than one mode of propagation. This coupling is manifested in the transmission spectrum by the existence impedance spikes, the locations of which is determined by grating characteristics as well as external factors such as temperature and strain. We can conclude from these considerations that the fiber grating sensors are based on a wavelength, or frequency, measurement.

In an optical fiber's core, a fiber Bragg grating [24] pairs forward-propagating light from a backward-propagating light mode. Therefore, $\beta_2 = -\beta_1$ and $\Delta\beta = 2\beta_1$, as a result, a length Λ is obtained in the order of micrometers [23]. The coupling takes place at a set of wavelengths known as Bragg wavelengths, which are defined as [25].

$$\lambda_{\text{Bragg}} = 2 n_{\text{eff}} \Lambda \quad (2.2)$$

where n_{eff} is the propagating core mode's effective refractive index. As shown in Figure 3, the propagation or mirrored spectrometry of an FBG show a narrow plunge or spike focused on λ_{Bragg} .

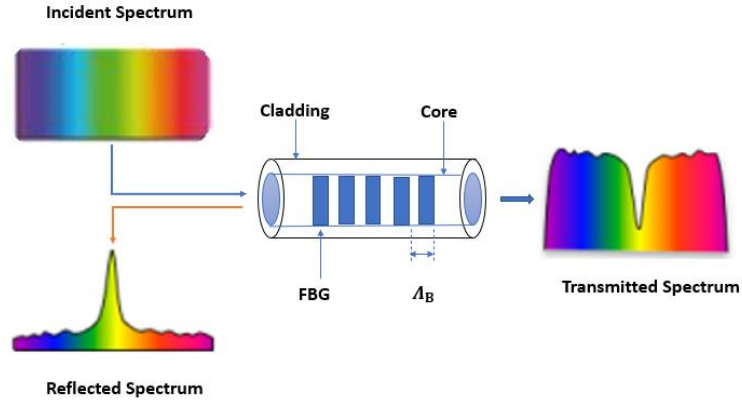


Figure 3. Spectra of an FBG

A Long Period Grating (LPG) allows to pair transmitting core mode light to a separated co-propagating cladding modes light of ordered equals to n . $\Delta\beta$ is negligible since $\beta_2 = \beta(n) > 0$. As a result, the period Λ is of magnitude of hundreds of micrometers [23] [26]. The grating's propagation spectrum consists of a collection of impedance bands because of the quickly attenuated cladding modes. Each band is corresponding to a distinct cladding mode coupling that focuses at a spectral range described by [26]:

$$\lambda(n) = \delta_{n_{eff}} \Lambda \quad (2.3)$$

where $\delta_{n_{eff}}$ is the difference between n_{eff} and $n_{clad}^{(n)}$, n_{eff} and are propagating core mode's refractive indices and $n_{clad}^{(n)}$ cladding mode's refractive indices. The impedance group spectral range is affected by a couple of exterior factors, including strain, temperature, and the diffraction coefficient of the center around cladding [27] [23].

In an apodized FBG, the profiles of gratings are not imprinted in a uniform manner. Modifying grating profile strength to realize more steady transitions among gratings is what this entails. Apodized gratings are nonuniformly modulated core gratings. Apodized grating configuration is used for eliminating side lobe in the spectral measurement [28]. In order to increase the spectrum's side lobe suppression ratio (SLSR), various apodization profiles have been investigated. Gaussian, Nuttall, and chirped apodization are examples of these profiles. In a research that uses a di-ureasil coating for humidity measurement, apodized grating profile with a Gaussian profile were used [29].

Via changing periodical profile in the refraction indices, FBG (CFBG) chirped gratings can be created [30]. Because the periodicity of the grating varies, CFBG reflects different spectra. The linear increase in FBG frequency alternation across the grating profile allows for wider spectral measurement compared with that of the conventional Bragg gratings [30]. An experiment involving utilization of chirped FBG for pressure-monitor system was recently published [31]. For gas-pressure monitor, chirped FBG is attached with rubbers, and then attach to a plate. The chirped FBG observed a comparatively excellent accuracy of -267.7 pm/kPa inside a detection spectrum of 0-10 kPa. The linear relationship of comparatively excellent accuracy pressure gauge is 97.93 percent, and smaller compared to that of metallic diaphragm and pressure gauge with 99.99 percent. The research shows that chirped FBG can be used as sensing element for low pressure, high sensitivity performance.

Tilted grating is a grating profile that is investigated most recently. In contrast to uniform or apodized gratings, the modulation of refraction indices has an oriented angle[32]. Tilted gratings are caused by a change in the refractive index of the fibre core when the grating plane and the fibre cross-section are tilted at an angle. Mode coupling becomes more complex as a result [33]. Tilted

gratings have been used for the development of gas composition sensors [34]. Researches found that ethanol and gasoline solutions could be detected successfully.

2.3 FBG Technology

As previously stated, a fiber Bragg grating is formed by an intense light interference pattern causing a regular modification of the reflectance coefficient in the fiber core. A little quantity of light guided along the fiber core is reflected at each different reflectance coefficient, and all of the reflections add up coherently at well-defined wavelengths called Bragg wavelengths, as defined in Hill et al. [25] were the first to show how permanent grating can be formed. They used 488 nm laser to excite a germania-doped optical fiber, and observed that the reflected light intensity raised over time, till nearly the total light was reflected back from the fiber. Photosensitivity, a non linear effect that realize the amplification of fiber core reflection coefficient using extensive laser pulse radiation to exposure and imprint the fiber, was used to explain the increase in back reflected light. A fiber Bragg grating was created in this early experiment when a little quantity of laser pulse mirrored back from the optical fiber's final interfered with the intense laser pulse to create a periodic pattern. When deliberate interference results in a optimum of laser pulse magnitude, the index of refraction increases to a greater extent. The reflected light becomes more intense as the grating's strength, which is correlated to the extent of its coefficient modulation, improves until it saturates.

The phase mask technique [35], which was successively introduced in 1993, largely replaced the fiber Bragg gratings imprinting approach. A phase mask is a shallow periodic rectangular wave structure with transparent and opaque regions that are etched into a thin slab of

silica glass using photolithographic techniques. The phase mask has a principle aim to separate the laser pulse to different orders of diffraction, namely 0, +1, and -1, one reason behind this goal is that the phase mask is made by silica which is translucent to UV light. Zero-order diffraction is suppressed by carefully controlling the phase mask's ridge deepness, allowing the order of positive/negative one of the diffraction laser pulse to meet the requirement for the production of the intense wave laser pulse that pass through the optical fiber core and thus can be used for inscription of Bragg gratings. The phase mask period will be half of the photon imprinted index grating period. The grating period is not affected by the wavelength of the writing radiation.

Several research teams were concerned with the development and creation of novel grating techniques using more complicated reflection coefficient modulation characteristics in the mid-1990s. as a result of technological assessment.

Chirped FBGs, apodized FBGs, phase shift FBGs, tilted FBGs, and long period fiber gratings are some examples [36] [37]. The industrial transformation took place in the middle of 1990s, spurred by telecommunications demands and the explosion of the communications balloon, a massive increase is seen in the corporations and research organizations involved in the optical fiber grating development, manufacturing, distribution, and deployment. In 1995, 3M, Photonetics, and Bragg Photonics were the first companies to commercialize FBGs. Many industry players made a significant shift from telecommunications to sensor industry shortly after telecommunications bubble burst. At the time, continuing to exploit the technical and manufacturing infrastructure was a wise and tactical decision in the segment of FBG industrial. The majority of optical sensing industry focused on discontinuous, singular sensor of particular specifications like temperature and strain, utilizing sensing system of concealed or packed gratings, as FBGs transitioned from telecommunications system to sensor components. lateral

radiation of interferometric methods or phase masks were commonly used to create these early gratings. Initially, the manufacturing procedures of these FBGs depends massively on manual labor, dramatically restricting the gratings' crucial characteristics and functionality regarding fabrication capability, reproducibility, structural durability and the amount of FBGs that can be written on a continuous fiber. Various experiments have been conducted in the development of opto-electronic elements capable of demodulating FBG-based sensors as a result of the growing interest in FBG sensing technology. The sensor industry, on the other hand, is significantly more cost-conscious, necessitating different sensor points and increased structural stability. The capability to manufacture a series of various FBGs at various regions of an optical fiber is also required. To meet these demands, increasingly advanced on-fly reel-to-reel manufacturing procedures and technologies are being designed, enabling the inprinting of intricate FBG rows onto an optical fiber. [38] [39].

External factors have an impact on the FBG reaction. Moreover, every alteration in grating structure or the reflective index, like temperature or strain , changes the Bragg spectrum, rendering the FBG an excellent intrinsic sensing element for wavelength-encoded data that is unaffected by the amplitude of signal [25]. If the grating has a force DF subjected, the sensing data changes in consistence with the equation below:

$$\frac{\Delta\lambda_{Bragg}}{\lambda_{Bragg}} = \left(1 + \frac{1}{n_{eff}} \frac{\delta n_{eff}}{\delta S} \right) \left(\frac{1}{\Lambda} \frac{\delta \Lambda}{\delta F} \right) \Delta F \quad (2.4)$$

where S stands for strain. For a grating with a wavelength of 1300 nm, a typical responsiveness to stretched lateral stress is 1 nm per millistrain [40]. When DT varies in temperature, the grating's central wavelength shifts according to the relationship:

$$\frac{\Delta\lambda_{Bragg}}{\lambda_{Bragg}} = \frac{1}{n_{eff}} \left(\frac{\delta n_{eff}}{\delta T} \right) \Delta T + \frac{1}{\Lambda} \left(\frac{\delta \Lambda}{\delta T} \right) \Delta T \quad (2.5)$$

where $\frac{\delta n_{eff}}{\delta T}$ is the thermo-optic coefficient, which is around 105/C [41], and $\frac{1}{\Lambda} \left(\frac{\delta \Lambda}{\delta T} \right)$ is the thermal expansion coefficient, which is around 0.5 106/C at room temperature [42].

The thermo-optic effect is primarily responsible for the thermal index of a grating at 1550 nm, which is around 0.01 nm per C. However, the performance is also dependent on the coating of fiber, specifically substance and coverage depth of the coating; moreover, as coverage becomes deeper, the saturation tendency increases [43]. When the spike of the grating locates at smaller wavelengths, sensitivity of temperature decreases as well [44].

2.4 Interrogation Techniques and Multiplexing for Quasi-Distributed FBGs

The interrogation system, which analyses the back-propagation data of FBGs, is the most crucial component of surveillance method regarding both quality and expense[45]. Minimal wattage, greater sensitivity, fast responsiveness, compact volume and the ability to carry fast data acquisition even in real-time manner are all requirements for FBG interrogation systems. To achieve all of these results, FBG sensing system necessitate the use of a costly optics sensor interrogator. Because of their high accuracy, Engineers have embraced FBG, making them the most popular sensing element for SHM. The FBG sensors' typical resolutions and measurement ranges are those required by civil engineering: The thermal working spectrum for stress analysis is in about ten me and greater than 200 C, with precision to be 1 e and 0.1 C, which corresponds to a spectral precision of around 1 pm. While this spectrum precision can be effortlessly realized by costly lab experimental instruments, resolving resolution within this range and compact, packed electro optics device that can be functional outside the lab could be more difficult.

The FBG interrogation approach chosen is determined by the optic parts method available in given utilization. Negative band illustration within telecommunication C bandwidth is the easiest approach to interrogate a fiber Bragg sensor series (1530-1565 nm). A one dimensional sensing series could be produced in a singular longer optic fibre by imprinting a series of FBGs containing distinct and separate Bragg wavelengths or through binding stubs of shared optic fibre to distinct FBGs.

The wavelength spacing of FBG sensors can be as small as 1 to 2 nanometers, enabling at most several dozens of them multiplexable within one C band optical fibre. Every optical fiber Bragg grating could be located along the optical fiber at any point. Crosstalk caused by numerous back-reflective signals and spectrum projection, however, ultimately determines the smallest separating distance and the most quantity of FBGs. As a result, the same optical fiber serves as a stress sensor array, one multiplexable setup, and a transmissible center all at the same time. This allows for multiple point sensing and quasi-distribution sensors to function. The system is fed with a pulse signal with a broad spectral signal including the wavelength of every Bragg grating, and a wavelength detecting device gets a narrow-band element mirrored from the FBGs. Time-division multiplex (TDM) and wave-division multiplex (WDM) are the two most common interrogation schemes. TDM systems use a square broad-band light to distinguish between distinct FBGs having equal Bragg frequencies based on how long it takes for each FBG's reflective light to get to the detecting device, with closer gratings receiving signals before those from further away. The frequency in every signal can be determined by its arrival to the detector. An alternative is by using a high-speed spectrometer. The requirement for small specular reflection FBGs of the tiny gap within them to allow the investigator sufficient period to obtain wavelength measurements are two major drawbacks of TDM systems. These drawbacks frequently limit a TDM measurement system's

performance and utility. Within the singular fibre various FBGs could be integrated and resolved at the same time using a WDM system, as long as the FBGs are distinct in wavelengths. In practice, it can be accomplished by combining a broad-band pulses with a spectral measuring device to detect, another approach is by combining basic photo-diode detecting device with configurable, swept-wavelength pulse power.

3.0 Reel to Reel System Design and Working Principle

In this section, we will present the components and layout of the reel-to-reel system in Section 3.1, the control algorithm and sample fabrication process in Section 3.2, and outcome of the fabricated sample scanned by OBR in Section 3.3.

3.1 Components and Layout

To accomplish the objectives, the preferable devices and hardware of the system have been evaluated and chosen among several different alternatives available in the market, which would generate the most desirable outcome considering the robustness of the system, the fabrication speed, accuracy, and cost.

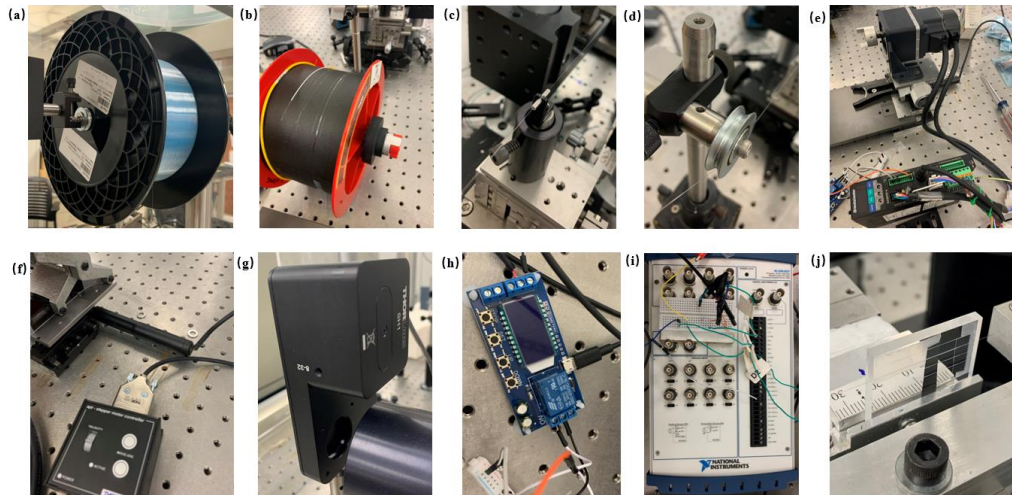


Figure 4. Reel-to-reel system components

As shown in Figure 4, the reel-to-reel system consists of two spools Figure 4(a) and Figure 4(b), the one in Figure 4(a) as feeder, and the other in Figure 4(b) as receiver, with each has a different adaptor, two ferrules are deployed and one of them is shown in Figure 4(c), two pulleys and their support structure are applied and one of them is shown in Figure 4(d), an Orientalmotor brushless motor of modal BXM230-GFS with gear head GFS2G200 of a reduction gear ratio 200 : 1, and its driver BXSD30-A are shown in Figure 4(e), a transversal Thorlabs actuator of modal ZST225B and its driver TST101 are shown in Figure 4(f), a Thorlabs shutter of modal SH1 and its driver KSC101 are shown in Figure 4(g), a phase mask, a timing relay and an NI digital I/O device of modal USB-6221 for communication are shown in Figure 4(j), Figure 4(h), and Figure 4(i), respectively.

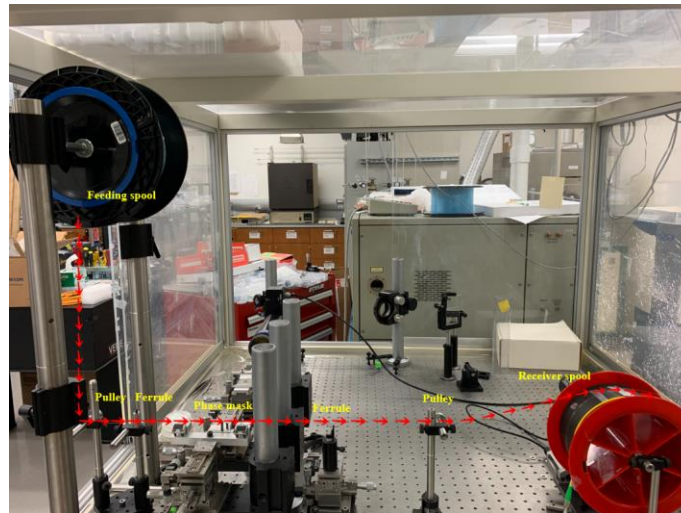


Figure 5. Reel-to-reel system layout

The overall component layout is shown in Figure 5. Firstly, the fiber sent from the feeding spool changes its direction through the pulley, then the fiber is aligned to position of phase mask by two ferrules, after the laser inscription, the fiber is transmitted to the receiver spool via the

second pulley. However, it is not as straightforward as it seems, to successfully inscribe FBG into the fiber core, the tension, the transversal and vertical displacements of the fiber need to be with in minimum variation while the fiber is being drew by the motor, if the fiber's tension is not steady, it is likely to cause about 2nm shift in the Bragg wavelength of the fabricated FBG [25]. Moreover, if the fiber moves transversally or vertically when being drew, it is likely to cause the fiber core to move out of the phase mask target region, resulting in inscription failure. To solve the problems of tension and movement variability, the preferable devices and hardware of the system have been evaluated and chosen, and the layout of each components are discreetly designed as explained below.

First, the ferrules located in both sides of the face mask are crucial to keep the fiber at desired location, their structure and cross section view are shown in Figure 6, the fiber used is of diameter 125 micrometers, and the ferrule's bore hole at the right end is 150 micrometers, by combining two ferrules, the fiber can be aligned while being drew by the motor with a minimum displacement. The ferrules have 60 degrees of angle as indicated in the cross section of Figure 6, which is important to keep the fiber from stuck in the ferrule and avoid fiber breaking, enabling smooth fiber transmission. To use the ferrule correctly, the fiber needs to be transmitted from the left to right, otherwise, the fiber will stuck by the sharp vertical angle and break. Apart from that, the grooves inscribed into the clamping place of the phase mask and the pulleys located near the reels are used to guide the fibers from one reel to another and facilitate the alignment and reduce vibration and displacement during fiber drawing.

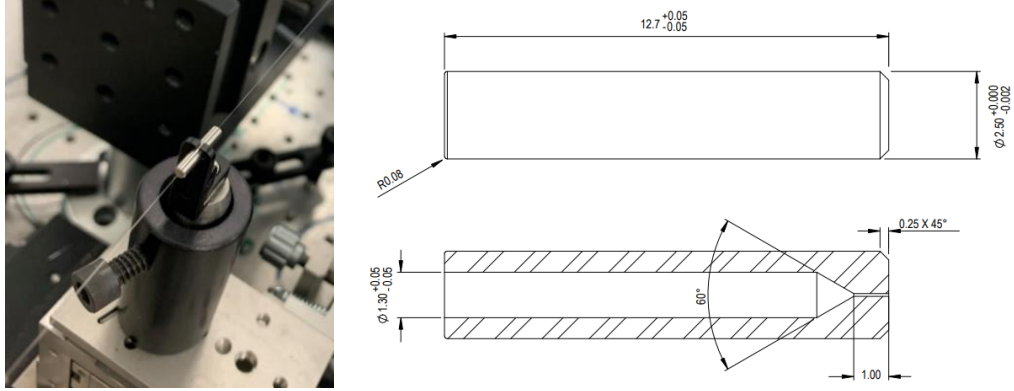


Figure 6. Ferrule structure

The displacement of the fiber is monitored using a camera with amplify capacity of three times as shown in Figure 7, the camera is placed above the phase mask and fiber, and the fiber begins to be transmitted, meanwhile, the camera is turned on and the real-time footage is shown in a 27-inch monitor, with the three times capacity, the result shows no noticeable displacement in transversal direction. As for the vertical direction, it is assumed that the probability of vibration and displacement is similar to the transversal displacement since the fiber is constrained by cylindrical ferrules, thus there is no necessity to monitor the vertical displacement.

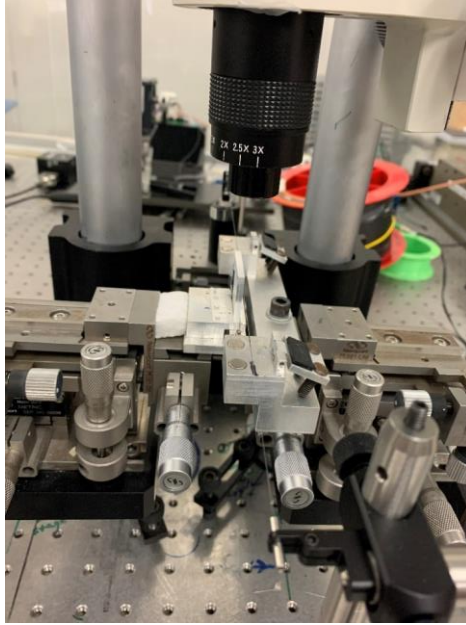


Figure 7. Top view of the fiber drawing displacement testing monitored by camera

To ensure steady fiber tension when the fiber is being drawn, the feeding reel needs resistance when being pulled, which can be realized by adding axial clamping force to the ball bearings the drum sits on. The axial clamping force would generate a friction between the drum and the adaptor, resulting in opposite force when the drum rotates, and this force is transmitted to the fiber in the form of tension. The ball bearing part connecting the adaptor and the reel is crucial, it resembles the structure of a classical two-bearing-one-shaft structure, the shaft ends are connected to a rigid supporter where the inner ring of the bearing sits on. On the other hand, the outer ring of the bearing rotates with the reel as the feeding reel rotates and feeds fiber. But the inner ring of the bearing stays still with the shaft since a screw and two washers are used to clamp both the inner rings to create friction, and thus control the tension, which can be adjusted manually. In addition, the reel needs to always rotate in the same direction with the screw fastening direction, otherwise it might be loose due to the friction, causing the assembled reel to collapse and damage the phase mask. By applying the mechanism of the tunable axial clamping force, the steady tension

of the fiber can be guaranteed, moreover, this design allows the tension to be adjustable using a nut.

To enable stable transmission of the fiber, the receiver reel is connected to the receiver motor in a rigid way via a 3D printing flange as shown in Figure 8 with its cross-section view, the flange connects the motor shaft to the spool using transition fit and is very tight to ensure the spool rotates simultaneously with the motor shaft. Apart from that, to avoid the problem of spool bending from the motor shaft by the gravity since the reel is one-end-connected, the other end of the reel needs to be supported by a stand which can hold a rotating spool.

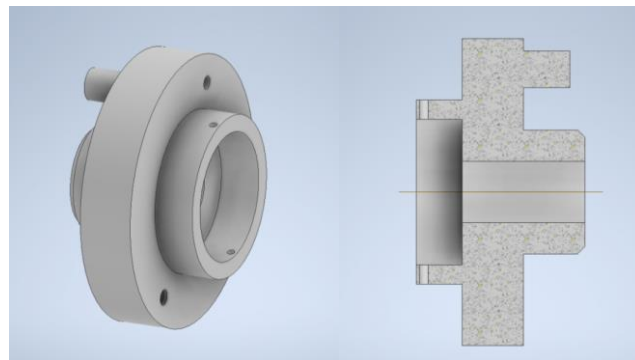


Figure 8. 3D printing flange with its cross-section view

The receiver motor is applied to pull the fiber of desired length in a suitable speed that the fragile fiber does not break, this is the primary requirement for the motor since the quasi-distributed FBG array needs to be evenly spaced. The length control is realized by controlling the time and speed motor runs, the time control is via the timing relay, and speed control is via the Orientalmotor software MEXE02 that can write the desired speed value to the motor driver and store it as operational data. In addition to speed, the operational data also includes parameters of motor acceleration and deceleration, which are crucial to avoid fiber break at the beginning of fiber

pulling, moreover, steady and small deceleration keeps the tension of the fiber constant and reduce the effect of the rotating momentums of the system.

If only the receiver motor is used, the circumference of the receiver reel will increase as more fiber are rolled in, but the total angle motor runs are constant, thus the length of each segment the motor collect increases more and more as the fiber length increase, which would be a problem, causing the FBGs cannot distributed evenly along the fiber. To solve the problem, a transverse motor is added and works together with the receiver motor to collect the fiber layer-by-layer onto the spool. The transverse motor is a Thorlabs linear actuator motor and is controlled by TST101 controller using kinesis. The transverse motor is used when large amount of fiber needs to be collected, to avoid too much fiber overlapping and causing error in the length of each segment. say, if 3 meters of fiber is wanted for each segment of sensor region, but the diameter of the spool increase as a result of more and more fiber overlap together as the motor rotate same angles for each collection, the actual length will be larger, if this error keeps increasing, the sensitized region will be more and more sparse. By adding a transversal motor, the error of the fiber length is reduced to minimum as the fiber is very thin, and it also expand the capacity of the fabrication to inscribe longer sensors in one time.

3.2 Control Algorithm and Fabrication Process

The system communication setup is very essential when developing a fully automated system with different components. There were no off-the-shelf answers and needs to build it step by step. As shown in Figure 9, the computer is connected NI I/O device via USB protocol to realize LabVIEW control, then the timing relay and shutter is connected to the NI I/O device, and the receiver motor is then controlled by the timing relay. Meanwhile, the transverse motor is connected to the computer via Software Kinesis and can be synchronized with the receiver motor.

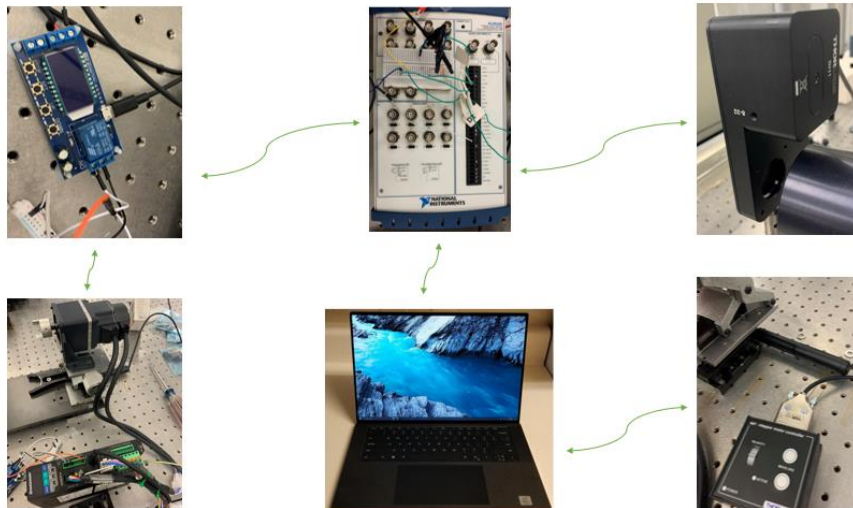


Figure 9. Reel-to-reel system communication setup

To realize fully automated control of the reel-to-reel system, LabVIEW is applied as the control center and the code's algorithm is shown in Figure 11. At the beginning of the fabrication, the parameters including the value of motor velocity, acceleration, and deceleration needs to be determined and written into the receiver motor's driver, the driver will store the data as operational data, and a circuitry, as shown in Figure 10, is connected to the I/O channel of the driver to select a specific set of operational data, then the parameters including the motor ON time, shutter ON

time, and total iterations needs to be determined and set in LabView. After the parameters has been encoded, the communication between PC and other I/O device needs to be connected, and the shutter needs to be in triggered mode to enable LabVIEW control. Last step of the preparation is to warmup the laser source and ensure the pulse strength is stable.

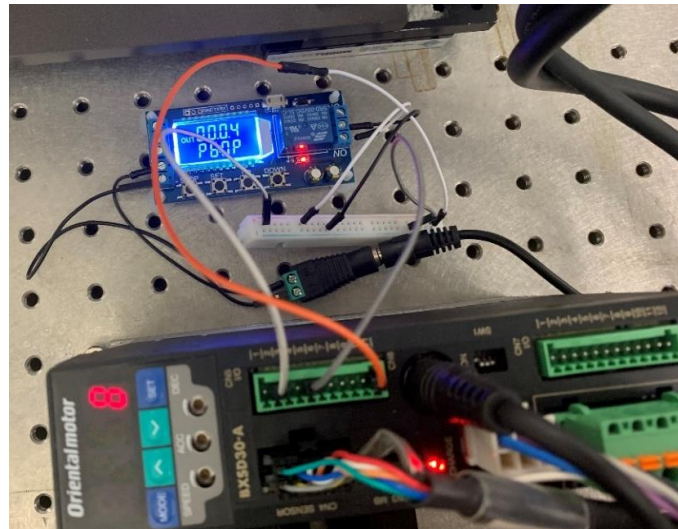


Figure 10. Circuitry of the motor driver

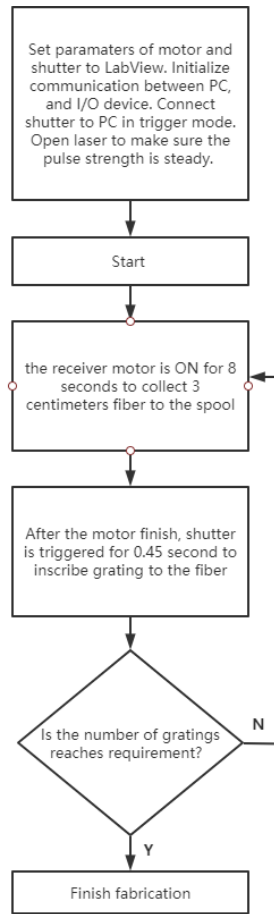


Figure 11. Reel-to-reel system control algorithm

Then start the fabrication process, first start the LabVIEW program to let NI USB6221 I/O device to activate the relay, as relay is ON and start timing, the motor receive the signal and start to accelerate, after reaching the desired rotational speed, it will take uniform motion until the programmed time is up, the timing relay tells the motor to stop, after the motor receive the stop signal, it will start to decelerate in a speed that has been written into the motor driver. After the motor speed becomes zero, the shutter will be trigger ON for a pre-set time around 0.45 second to make sure the fiber core can be radial imprinted for at least one pulse of UV laser through the phase mask, since the UV excimer laser source could generate UV pulses of period around 0.2 second. Successively, the shutter will be closed, shutting out the laser beam to stop grating

inscription. The receiver motor would then start to rotate and collect the imprinted FBG to the spool. This would be one full circle to fabricate an FBG grating, and it can be repeated to fabricate more FBGs needed, as a result, every FBGs will be fabricated and ensured to be evenly distributed along one fiber.

3.3 Fabrication Results

The sample fabricated is tested via an Optical Backscatter Reflectometry (OBR), the return loss is measured regarding the distance, as can be seen from Figure 12, the loss profile is evenly spaced three centimeters apart, which is exactly the desired distance, as the yellow and red marks has a displacement of 59 milliliters, given the error in manual measurement, the distance between each inscribed FBG should be evenly spaced in 3 centimeters as desired. Apart from the horizontal axis, the vertical axis shows the amplitude of the back scattering signal including Fresnel reflection and Rayleigh backscattering, and the segment has a steady amplitude which is around -80 dB, which means the FBGs has a similar reflectivity. However, in order to obtain more details about the FBGs, their peak wavelength and corresponding reflectivity are calculated via OBR using Fourier transform.



Figure 12. OBR scanning result

For each of the 150 fabricated FBGs, their peak wavelength and corresponding reflectivity are collected. The peak wavelength of the 150 FBGs are concentrated between 1548.3 nm to 1549.3 nm, as shown in Figure 13, and their corresponding reflectivity are around -30 dB as shown in Figure 14. Although some of the inscribed FBGs have bias in reflectivity, the majority of the FBGs are of constant peak wavelength and reflectivity with acceptable bias. The deviations in reflectivity of certain FBGs might be due to the intrinsic instability of the laser strength, or it could be due to the small variation of the tension in the fiber between each inscription as a result of friction between fiber and spool, ferrule and pulley.

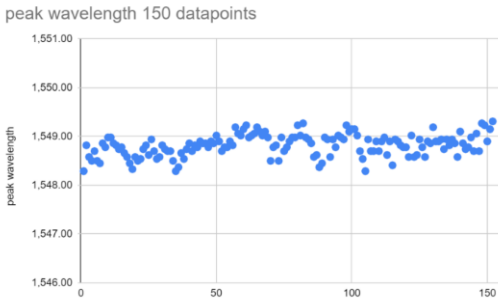


Figure 13. Peak wavelength of the fabricated sample

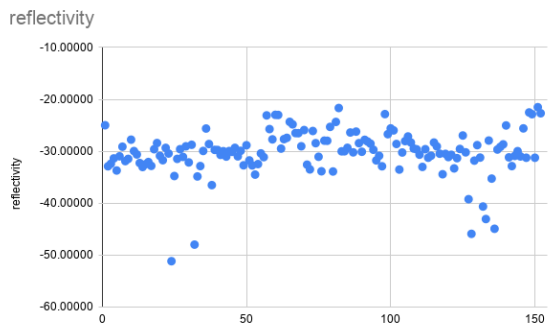


Figure 14. Corresponding reflectivity of the fabricated sample

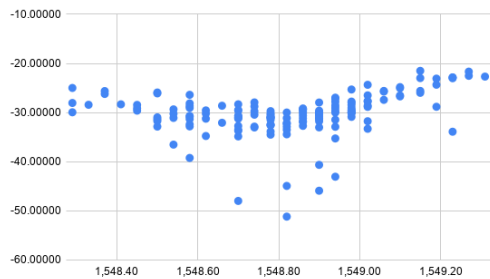


Figure 15. Combination of peak wavelength with corresponding reflectivity of the fabricated sample

As can be seen from the combination of peak wavelength with corresponding reflectivity of the fabricated sample in Figure 15, most of the points are concentrated whereas less than 4 percent of the FBGs has a reflectivity below -40 dB, all of these devious points are located near the peak wavelength of 1548.8 nm.

4.0 Summary and Future Works

In this section, we will present the summary of the thesis in Section 4.1, and the future works in Section 2.4.

4.1 Summary

The fabrication and testing of quasi-distributed FBG sensors are the focus of two major works in this thesis: one aims to develop a reel-to-reel system that significantly improves the efficiency and accuracy of quasi-distributed FBG sensors fabrication using small diameter single-mode optical fiber in [1], and the other focuses on testing the fabricated sensor via OBR.

To begin, a fully automated reel-to-reel system, which in its entirety embedded 2 motors, fiber guidance system, fiber feeder and collector, and various sensors, is designed and integrated into the laser system to address the problem of manually fabricating quasi-distributed fiber sensors. This allows evenly spaced gratings to be inscribed continuously along an optical fiber. Two motors, fiber guidance, alignment, and supports, two spools for fiber feeding and collection are crucial parts of the system.

LabVIEW allows the system to control the speed and distance. Meanwhile, to overcome the effect of momentum and achieve stable tension, the motor is controlled to have constant acceleration and deceleration.

The reel-to-reel system is put to the test, with 150 FBGs inscribed along a single fiber. Because the total time spent is less than an hour, manual fabrication's speed limitations are no longer an issue. Because the fiber is fed and collected on two large spools, the length of the fiber has no bearing on the handling risk of breaking off the fiber, and the distance limit is also exceeded in the system.

Furthermore, the samples fabricated by the reel-to-reel system are scanned by OBR, and the results show that each FBG is spaced evenly with three centimeters, and their Bragg waveforms are very close, demonstrating that the manual fabrication precision limitations have been overcome.

4.2 Future Works

In this thesis, only quasi-distributed FBGs samples have been fabricated. Future studies will focus on the sample's real application performance such as acoustic sensing, vibration sensing or temperature sensing.

Besides, in this paper, the fabrication results scanned by OBR indicates the possibility of variance in the reflectivity, which might be due to the instability in laser pulse intensity, or the variation in fiber tension during fiber drawing. The two factors should be investigated, and a mechanism should be designed to avoid the effect of both factors, which will lead to better FBGs fabrication.

Another direction for future work is to improve the controllability of the reel-to-reel system regarding the compatibility of the fiber used in this system. Now only the small diameter fiber

used is proved to be feasible, however, for fabrication of FGBs from normal single mode optical fibers, the jacket of the fiber needs to be removed, as a result, the fiber used is more fragile, and the jacket-removed part of fiber might get stuck in the ferrule during fiber drawing, inducing fiber breakage. So the future work can focus on improving the reel-to-reel system with more compatible fibers by using a better designed ferrule together with more delicate fiber drawing process that enable more fragile fibers to be drawn in this system.

Bibliography

- [1] J. Wu *et al.*, “Fabrication of Ultra-Weak Fiber Bragg Grating (UWFBG) in Single-Mode Fibers through Ti-Doped Silica Outer Cladding for Distributed Acoustic Sensing,” *Opt. InfoBase Conf. Pap.*, vol. Part F172-, no. c, pp. 4–5, 2019, doi: 10.1364/es.2019.eth1a.4.
- [2] A. G. Mignani *et al.*, “EAT-by-LIGHT: Fiber-optic and micro-optic devices for food quality and safety assessment,” *IEEE Sens. J.*, vol. 8, no. 7, pp. 1342–1354, 2008, doi: 10.1109/JSEN.2008.926971.
- [3] A. G. Mignani and F. Baldini, “Fibre-optic sensors in health care,” *Phys. Med. Biol.*, vol. 42, no. 5, pp. 967–979, 1997, doi: 10.1088/0031-9155/42/5/015.
- [4] H. Lamela, D. Gallego, R. Gutierrez, and A. Oraevsky, “Interferometric fiber optic sensors for biomedical applications of optoacoustic imaging,” *J. Biophotonics*, vol. 4, no. 3, pp. 184–192, 2011, doi: 10.1002/jbio.201000096.
- [5] Y. Yang, V. G. M. Annamdas, C. Wang, and Y. Zhou, “Application of multiplexed FBG and PZT impedance sensors for health monitoring of rocks,” *Sensors*, vol. 8, no. 1, pp. 271–289, 2008, doi: 10.3390/s8010271.
- [6] Y. Kawabata, T. Kamichika, T. Imasaka, I. Nobuhiko, “Fiber-optic sensor for carbon - dioxide with a ph indicator dispersed in a poly(ethylene glycol) membrane”, *Analytica Chimica Acta*, 219, 223-229, 1989, doi: 10.1016/S0003-2670(00)80353-0.
- [7] V. G. M. Annamdas, Y. Yang, and H. Liu, “Current developments in fiber Bragg grating sensors and their applications,” *Sensors Smart Struct. Technol. Civil, Mech. Aerosp. Syst. 2008*, vol. 6932, no. March, p. 69320D, 2008, doi: 10.1117/12.775715.
- [8] H. Y. Fu *et al.*, “Pressure sensor realized with polarization-maintaining photonic crystal fiber-based Sagnac interferometer,” *Appl. Opt.*, vol. 47, no. 15, pp. 2835–2839, 2008, doi: 10.1364/AO.47.002835.
- [9] TSY. Francis, Y. Shizhuo, BR. Paul. “Fiber Optics sensors” CRC Press, Optical science and engineering, 132, 2008
- [10] B. Gu, M.-J. Yin, A. P. Zhang, J.-W. Qian, and S. He, “Low-cost high-performance fiber-optic pH sensor based on thin-core fiber modal interferometer,” *Opt. Express*, vol. 17, no. 25, p. 22296, 2009, doi: 10.1364/oe.17.022296.
- [11] V. G. M. Annamdas, “Review on Developments in Fiber Optical Sensors and Applications,” *Int. J. Mater. Eng.*, vol. 1, no. 1, pp. 1–16, 2012, doi: 10.5923/j.ijme.20110101.01.

- [12] S. Sumitro, M. Tominaga and Y. Kato “Monitoring Based Maintenance for Long-Span Bridges,” First International Conference on Bridge Maintenance, Safety and Management, 14-17 July, Barcelona, Spain, 2002.
- [13] G. Rajan, Optical Fiber Sensor: advanced technique and applications. CRC press, 2015
- [14] E. J. Udd, Corones and H.M. Laylor “Fiber optic sensors for infrastructure applications”, Final Report, SPR 374, February 98, Oregon Department of Transportation, and Federal Highway Administration, 1998
- [15] E. Udd, (1991). Editor, “Fiber Optic Sensors”, An Introduction for Engineers and Scientists. John Wiley and Sons, New York, USA
- [16] A. D. Kersey, Author, E. Udd, Editor. (1991). “Distributed and Multiplexed Fiber Optic Sensors”, Fiber Optic Sensors: An Introduction for Engineers and Scientists. Wiley. New York
- [17] H. Bartko, F. Goebel, R. Mirzoyan, W. Pimpl, and M. Teshima, “Tests of a prototype multiplexed fiber-optic ultra-fast FADC data acquisition system for the MAGIC telescope,” *29th Int. Cosm. Ray Conf. ICRC 2005*, vol. 5, no. September 2018, pp. 167–170, 2005, doi: 10.1016/j.nima.2005.05.029.
- [18] N. Mrad and G. Z. Xiao, “Multiplexed fiber bragg gratings for potential aerospace applications,” *Proc. - 2005 Int. Conf. MEMS, NANO Smart Syst. ICMENS 2005*, pp. 359–363, 2005, doi: 10.1109/ICMENS.2005.79.
- [19] F. Ansari, “Practical implementation of optical fiber sensors in civil structural health monitoring,” *J. Intell. Mater. Syst. Struct.*, vol. 18, no. 8, pp. 879–889, 2007, doi: 10.1177/1045389X06075760.
- [20] L. Yuan and Y. Dong, “Multiplexed fiber optic twin-sensor array based on a combination of mach-zehnder and michelson interferometers,” *J. Intell. Mater. Syst. Struct.*, vol. 20, no. 7, pp. 809–813, 2009, doi: 10.1177/1045389X08097955.
- [21] S. Addanki, I. S. Amiri, and P. Yupapin, “Review of optical fibers-introduction and applications in fiber lasers,” *Results Phys.*, vol. 10, no. July, pp. 743–750, 2018, doi: 10.1016/j.rinp.2018.07.028.
- [22] A. D. Kersey *et al.*, “Fiber grating sensors,” *J. Light. Technol.*, vol. 15, no. 8, pp. 1442–1462, 1997, doi: 10.1109/50.618377.
- [23] V. Bhatia and A. M. Vengsarkar, “Optical fiber long-period grating sensors,” *Optics letters*, vol. 21, no. 9, pp. 692–694, 1996.
- [24] R. Kashyap, Fiber Bragg Gratings. Academic press, second ed., 2009.
- [25] K. O. Hill and G. Meltz, “Fiber Bragg grating technology fundamentals and overview,” *Journal of lightwave technology*, vol. 15, no. 8, pp. 1263–1276, 1997.

- [26] A. M. Vengsarkar, P. J. Lemaire, J. B. Judkins, V. Bhatia, T. Erdogan, and J. E. Sipe, "Long period fiber gratings as band-rejection filters," *Journal of lightwave technology*, vol. 14, no. 1, pp. 58–65, 1996.
- [27] S. W. James and R. P. Tatam, "Optical fibre long-period grating sensors: characteristics and application," *Measurement science and technology*, vol. 14, no. 5, p. R49, 2003.
- [28] C. Campanella, A. Cuccovillo, C. Campanella, A. Yurt, and V. Passaro, "Fibre Bragg grating based strain sensors: Review of technology and applications," *Sensors*, vol. 18, no. 9, p. 3115, 2018.
- [29] S. F. H. Correia et al., "Optical fiber relative humidity sensor based on a FBG with a diureasil coating," *Sensors*, vol. 12, no. 7, pp. 8847–8860, 2012.
- [30] D. Tosi, "Review of chirped fiber Bragg grating (CFBG) fiber-optic sensors and their applications," *Sensors*, vol. 18, no. 7, p. 2147, 2018.
- [31] E. Vorathin, Z. M. Hafizi, A. M. Aizzuddin, M. K. A. Zaini, and K. S. Lim, "Temperature-independent chirped FBG pressure transducer with high sensitivity," *Opt. Lasers Eng.*, vol. 117, pp. 49–56, Jun. 2019.
- [32] T. Guo et al., "Highly sensitive detection of urinary protein variations using tilted fiber grating sensors with plasmonic nanocoatings," *Biosensors Bioelectron.*, vol. 78, pp. 221–228, Apr. 2016.
- [33] X. Dong, H. Zhang, B. Liu, and Y. Miao, "Tilted fiber Bragg gratings: Principle and sensing applications," *Photonic Sensors*, vol. 1, no. 1, pp. 6–30, Mar. 2011.
- [34] S. Aristilde, C. M. B. Cordeiro, and J. H. Osório, "Gasoline quality sensor based on tilted fiber Bragg gratings," *Photonics*, vol. 6, no. 2, p. 51, 2019.
- [35] K. O. Hill, B. Malo, F. Bilodeau, D. Johnson, and J. Albert, "Bragg gratings fabricated in monomode photosensitive optical fiber by UV exposure through a phase mask," *Applied Physics Letters*, vol. 62, no. 10, pp. 1035–1037, 1993.
- [36] B. Malo, J. Albert, K. Hill, F. Bilodeau, D. Johnson, and S. Theriault, "Enhanced photosensitivity in lightly doped standard telecommunication fibre exposed to high fluence ArF excimer laser light," *Electronics Letters*, vol. 31, no. 11, pp. 879–880, 1995.
- [37] T. Erdogan and J. Sipe, "Tilted fiber phase gratings," *JOSA A*, vol. 13, no. 2, pp. 296–313, 1996.
- [38] G. C. Righini, A. Tajani, and A. Cutolo, *An introduction to optoelectronic sensors*, vol. 7. World Scientific, 2009.
- [39] A. Cusano, A. Cutolo, and J. Albert, *Fiber Bragg grating sensors: recent advancements, industrial applications and market exploitation*. Bentham Science Publishers, 2011.

- [40] K. Hill, Y. Fujii, D. C. Johnson, and B. Kawasaki, "Photosensitivity in optical fiber waveguides: Application to reflection filter fabrication," *Applied physics letters*, vol. 32, no. 10, pp. 647–649, 1978.
- [41] I. Malitson, "Interspecimen comparison of the refractive index of fused silica," *Journal of the Optical Society of America*, vol. 55, no. 10, pp. 1205–1209, 1965.
- [42] A. D. Kersey, "A review of recent developments in fiber optic sensor technology," *Optical fiber technology*, vol. 2, no. 3, pp. 291–317, 1996.
- [43] Y. Li, Z. Hua, F. Yan, and P. Gang, "Metal coating of fiber Bragg grating and the temperature sensing character after metallization," *Opt. Fiber Technol.*, vol. 15, no. 4, pp. 391–397, 2009, doi: 10.1016/j.yofte.2009.05.001.
- [44] K. Krebber, H. Henschel, and U. Weinand, "Fibre Bragg gratings as high dose radiation sensors?," *Measurement Science and Technology*, vol. 17, no. 5, p. 1095, 2006.
- [45] Y.-J. Rao, "Recent progress in applications of in-fibre Bragg grating sensors," *Optics and lasers in Engineering*, vol. 31, no. 4, pp. 297–324, 1999.
- [46] A. M. Vengsarkar, P. J. Lemaire, J. B. Judkins, V. Bhatia, T. Erdogan, and J. E. Sipe, "Long period fiber gratings as band-rejection filters," *J. Lightw. Technol.*, vol. 14, no. 1, pp. 58–65, Jan. 1996.
- [47] E. Vorathin, Z. M. Hafizi, A. M. Aizzuddin, M. K. A. Zaini, and K. S. Lim, "Temperature-independent chirped FBG pressure transducer with high sensitivity," *Opt. Lasers Eng.*, vol. 117, pp. 49–56, Jun. 2019.
- [48] B. Jiang et al., "Graphene oxide-deposited tilted fiber grating for ultrafast humidity-sensing and human breath monitoring," *Sens. Actuators B, Chem.*, vol. 293, pp. 336–341, Aug. 2019.
- [49] C. Campanella, A. Cuccovillo, C. Campanella, A. Yurt, and V. Passaro, "Fibre Bragg-grating based strain sensors: Review of technology and applications," *Sensors*, vol. 18, no. 9, p. 3115, 2018.
- [50] Y. Qi et al., "Research on temperature and humidity sensing characteristics of cascaded LPFG-FBG," *Optik*, vol. 188, pp. 19–26, Jul. 2019.